

Kinetics of Formation of Ca^{2+} Complexes of Acyclic and Macrocyclic Poly(amino carboxylate) Ligands: Bimolecular Rate Constants for the Fully-Deprotonated Ligands Reveal the Effect of Macrocyclic Ligand Constraints on the Rate-Determining Conversions of Rapidly-Formed Intermediates to the Final Complexes

Shu Ling Wu, Kenneth A. Johnson, and William DeW. Horrocks, Jr.*

Departments of Chemistry and Biochemistry and Molecular Biology, The Pennsylvania State University, University Park, Pennsylvania 16802

Received May 30, 1996[⊗]

The apparent bimolecular rate constants, k_1 ($\text{M}^{-1} \text{s}^{-1}$), for the formation of Ca^{2+} complexes of a series of acyclic (edta, egta, cdta) and macrocyclic (dota, teta, do3a) poly(amino carboxylate) ligands were determined in the pH range 7–13 using the fluorescent ligand quin2 in a stopped-flow apparatus to monitor the ligand competition reaction. The k_1 values are observed to reach maximum constant values at high pH, characteristic of reactions involving the fully-deprotonated ligand species. Bimolecular formation constants $k_{\text{Ca}^{\text{L}}}$, $k_{\text{Ca}^{\text{HL}}}$, and $k_{\text{Ca}^{\text{H}_2\text{L}}}$, characteristic of the reaction of the fully-deprotonated and mono- and diprotonated ligands, respectively, were derived from the pH dependence of the k_1 values. The $k_{\text{Ca}^{\text{L}}}$ values of the acyclic ligands are edta, $4.1 \times 10^9 \text{ M}^{-1} \text{ s}^{-1}$; egta, $2.1 \times 10^9 \text{ M}^{-1} \text{ s}^{-1}$; and cdta, $2.3 \times 10^9 \text{ M}^{-1} \text{ s}^{-1}$, while the corresponding values for the macrocyclic ligands are dota, $4.7 \times 10^7 \text{ M}^{-1} \text{ s}^{-1}$; teta, $1.1 \times 10^7 \text{ M}^{-1} \text{ s}^{-1}$; and do3a, $1.0 \times 10^8 \text{ M}^{-1} \text{ s}^{-1}$. The smaller values for the macrocyclic ligands are consistent with ligand-dictated constraints imposed on the conversion of a stable intermediate to the final complex, a process which involves the simultaneous stripping of several water molecules from the first-coordination sphere of the Ca^{2+} ion.

Introduction

The influence of the structure of multidentate amino carboxylate ligands on the kinetics of their complexation with metal ions is a topic of fundamental interest and one with practical consequences for metalloenzyme therapy and diagnostic chelate treatment.^{1,2} For acyclic poly(amino carboxylate) ligands, most complexation reactions are extremely rapid with formation rate constants, k_f , greater than $\sim 10^8 \text{ M}^{-1} \text{ s}^{-1}$. Although there is only fragmentary evidence for the existence of discrete intermediates in complexation reactions of acyclic ligands,^{3,4} macrocyclic ligands such as those involving 9- to 14-membered tri- or tetraaza rings and three or four carboxylate-bearing side chains exhibit relatively slow rates of complexation.^{5–11} Indeed, relatively-stable intermediates have been directly observed using $^7\text{F}_0 \rightarrow ^5\text{D}_0$ luminescence excitation spectroscopy of Eu^{3+} in the cases of formation of complexes with dota,¹² do3a,¹³ and teta¹³ with this ion. Such an intermediate has also been observed by absorption spectroscopy in the Ce^{3+} –dota system.⁷ The exist-

ence of stable intermediates suggests that ligand structure and conformational constraints play an important role in determining the rates of formation reactions. On the basis of a recent study, we¹² proposed that the rate-determining step in the Eu^{3+} –dota system is the entry of the metal ion into the cavity of the macrocyclic ligand. Protonation of ring nitrogen atoms appears to hinder conversion to the final product by blocking inversion of configuration at the ring nitrogens. The detailed mechanism that we suggested involves OH^- ion-induced removal of protons from the ring nitrogens. Our suggested mechanism goes further than the widely-used empirical mechanism wherein k_{obs} is directly proportional to the hydroxide ion concentration at all pH values. Our mechanism predicts that the formation rate will reach a limit at high pH values where protonated species no longer exist.

Most kinetic studies of complexation reactions of this type have been carried out over a relatively-narrow region of low pH values where the free ligands exist predominately in protonated forms. The lower complexation rates of protonated species and the necessary deprotonation reactions have tended to obscure any differences in complexation rates among fully-deprotonated ligand species.^{9,11} This has left unclear the effect of ligand structure and rigidity on formation rate constants.

In order to assess these effects, it is necessary to work in a higher pH range (pH 11–13) where the ligands become fully deprotonated. This is impossible with lanthanide ions owing to the formation of insoluble hydroxides. Therefore, in the present work, Ca^{2+} is used as the metal ion, and complex formation is monitored by use of the well-studied fluorophoric chelator quin2, which is almost entirely deprotonated at pH values greater than 7.^{14,15} Our experiments involve a competition between Ca^{2+} binding to the multidentate ligand of interest

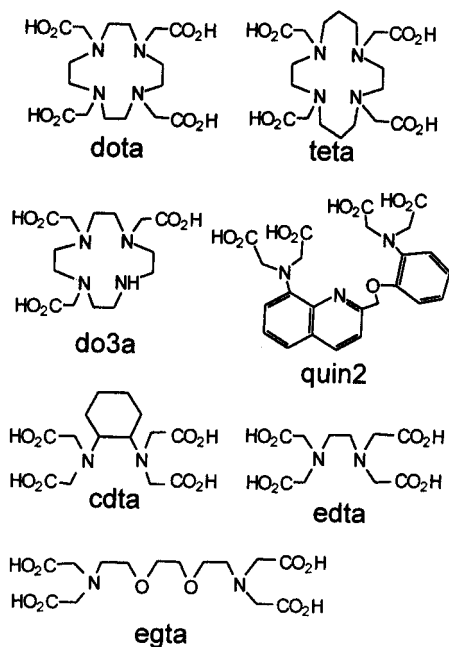
[⊗] Abstract published in *Advance ACS Abstracts*, March 15, 1997.

- (1) Cox, B. G.; Schneider, H. *Coordination and Transport Properties of Macrocyclic Compounds in Solution*; Elsevier: New York, 1992.
- (2) Margerum, D. W.; Cayley, G. R.; Weatherburn, D. C.; Pagenkopf, G. K. In *Coordination Chemistry*; Martell, A. E., Ed.; American Chemical Society: Washington, DC, 1978; Vol. 2, pp 1–220.
- (3) Carr, J. D.; Swartzager, J. *J. Am. Chem. Soc.* **1975**, *97*, 315–321.
- (4) Nyssen, G. A.; Margerum, D. W. *Inorg. Chem.* **1970**, *9*, 1814–1820.
- (5) Brucher, E.; Cortes, S.; Chavez, F.; Sherry, A. D. *Inorg. Chem.* **1991**, *30*, 2092–2097.
- (6) Kasprzyk, S. P.; Wilkins, R. G. *Inorg. Chem.* **1982**, *21*, 3349–3352.
- (7) Brucher, E.; Laurency, G.; Makra, Z. *Inorg. Chim. Acta* **1987**, *139*, 141–142.
- (8) Brucher, E.; Sherry, A. D. *Inorg. Chem.* **1990**, *29*, 1555–1559.
- (9) Kumar, K.; Tweedle, M. F. *Inorg. Chem.* **1993**, *32*, 4193–4199.
- (10) Wang, X.; Jin, T.; Comblin, V.; Lopez-Mut, A.; Merciny, E.; Desreux, J. F. *Inorg. Chem.* **1992**, *31*, 1095–1099.
- (11) Kumar, K.; Jin, T.; Wang, X.; Desreux, J. F.; Tweedle, M. F. *Inorg. Chem.* **1994**, *33*, 3823–3829.
- (12) Wu, S. L.; Horrocks, W. D., Jr. *Inorg. Chem.* **1995**, *34*, 3724–3732.
- (13) Wu, S. L.; Horrocks, W. D., Jr. To be published.

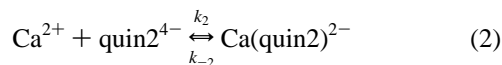
(14) Tsiens, R. Y. *Biochemistry* **1980**, *19*, 2396–2404.

(15) Quast, U.; Labhardt, A. M.; Doyle, V. M. *Biochem. Biophys. Res. Comm.* **1984**, *123*, 604–611.

Chart 1



L (eq 1) and Ca²⁺ binding to quin2 (eq 2). The ligands studied using a fluorescence stopped-flow technique¹⁶ are edta, egta, cdta, do3a, and teta (see Chart 1). In eq 1 k_1 and k_{-1} are the



apparent formation and dissociation rate constants, respectively, of CaL while k_2 and k_{-2} are the analogous constants for Ca(quin2)²⁻.

Experimental Section

Materials. Edta (98%), egta (99%), cdta (97%), teta, quin2, tetramethylammonium chloride (97%), and caps (99%) (3-(cyclohexylamino)-1-propanesulfonic acid) were purchased from Aldrich Chemical Co. Hepes (N-[2-hydroxyethyl]piperazine-N'-[2-ethanesulfonic acid]) and piperazine were purchased from Sigma. CaCl₂·2H₂O (99%) was purchased from EM Science. do3a and dota were provided by the Nycomed-Salutar Co. The water used was distilled and deionized. All chemicals were used without further purification. A CaCl₂ stock solution was prepared at ~0.05 M and standardized by an edta arsenazo titration. Stock solutions ~0.1 M in the individual ligands were prepared at a pH of approximately 10.

Kinetic Measurements. All kinetic measurements were performed by using a stopped-flow apparatus (Model SF-2001) built by KinTek Instruments Corp. (State College, PA). The mixing dead time is about 2 ms. Reactions were followed by excitation at 339 nm, and the emitted light ($\lambda > 455$ nm) was observed using a 450 nm cutoff filter. The apparent dissociation rate constant of Ca(quin2)²⁻, k_{obs} , was obtained by recording about three to six individual shots after which the data were averaged. These data were fit to a single-exponential function (Peakfit Program, Jandel Scientific).

All studies were carried out at 25 °C and ionic strength of 0.5 M with (CH₃)₄NCl as an added electrolyte. Typically, the reaction was initiated by mixing ligand and buffer (50 mM) in one syringe of the stopped-flow apparatus with quin2, Ca²⁺, and buffer (50 mM) in the other syringe at the appropriate pH. Unless specifically stated

otherwise, all of the concentrations reported are the concentrations after mixing. Both quin2 and ligand are in excess concentration over the total Ca²⁺ (5 μM) in each run in order to obtain pseudo-first-order kinetics. The buffers used were Hepes (pH 7–8), piperazine (pH 9–10), and Caps (pH 10–11). For pH values greater than 12, the solution has a strong self-buffering capacity; therefore, no buffer was used in this pH region.

Results

Determination of the Apparent Formation Rate Constant, k_1 . The formation rate constants for poly(amino carboxylate) ligand complexes of Ca²⁺ are too large to measure at the high pH values necessary to achieve full deprotonation of the ligand species. It was thus necessary to introduce a second chelator, quin2, to make a competitive system. The kinetics of this fluorescent indicator are well-known, and the fully-deprotonated ligand quin2⁴⁻ predominates in solution at pH values above 7.^{14,15}

At higher pH's the Ca²⁺ of eqs 1 and 2 represents the three species Ca²⁺(aq), Ca(OH)⁺(aq), and Ca(OH)₂(aq).^{18,19} Although the kinetics of complexation of the ligands in question with Ca(OH)⁺ or Ca(OH)₂(aq) are unknown, it is shown below that the relative formation rate constants, (k_1/k_2), can still be determined under conditions of high pH. Furthermore, L in eq 1 represents whatever mixture of protonated and fully-deprotonated ligand species that exists at a particular pH value. The two approaches taken to determine k_1/k_2 are described below.

Method 1: Measurement of the Apparent Dissociation Rate Constant of Ca(quin2)²⁻, k_{obs} , in the Presence of a Competing Ligand, L. Under conditions where both quin2 and L are in excess over total Ca²⁺, the free Ca²⁺ ion concentration is close to zero, and utilizing the steady state approximation for [Ca²⁺], k_{obs} is given by eq 3; see the Appendix

$$k_{\text{obs}} = \frac{k_{-2}(k_1/k_2)([L]_t/[quin2]_t) + k_{-1}}{(k_1/k_2)([L]_t/[quin2]_t) + 1} \quad (3)$$

in the Supporting Information. The total fluorescence intensity, $I(t)$, partitioned between that due to Ca²⁺-bound and free quin2 is given by eq 4

$$I(t) = k'[\text{Ca}(\text{quin2})^{2-}] + k''[\text{quin2}] = I(0) \exp(-k_{\text{obs}}t) + I_{\infty} \quad (4)$$

where k' and k'' are proportionality constants between fluorescence intensity and concentration.

In eq 3, [quin2]_t and [L]_t represent total concentrations of quin2 and L, respectively. $I(0)$ is the fluorescence intensity due to Ca(quin2) at $t = 0$. Since free quin2 is in large excess in all of our experiments, [quin2] is effectively constant and any fluorescence due to it, as well as any dark current, is represented by the constant I_{∞} .

Equation 3 reveals that measurement of k_{obs} as a function of [L]_t/[quin2]_t allows the determination of k_{-2} and k_1/k_2 . As an example, Figure 1 shows plots of the time course of the fluorescence intensity from Ca(quin2)²⁻ following mixing of Ca²⁺ and quin2 in one syringe with three different concentrations of dota in the second syringe at pH 13.02. The traces of Figure 1 are well-fit by eq 4, yielding k_{obs} and $I(0)$ values. Similar experiments were carried out with the other ligands involved in this study at a number of pH values greater than 7. Figure 2 reveals that k_{obs} asymptotically approaches a maximum value

(16) Johnson, K. A. *Transient-State Kinetic Analysis of Enzyme Reaction Pathway*, *The Enzymes*; Academic Press, Inc.: New York, 1992; Vol. XX, pp 1–61.

(17) $\alpha_L = 1/(1 + K_1^H[H] + K_1^H K_2^H[H]^2 + \dots)$; $\alpha_{HL} = \alpha_L K_1^H[H]$; $\alpha_{H_2L} = \alpha_L K_1^H K_2^H[H]^2$.

(18) Smith, R. M.; Martell, A. E. *NIST Critical Stability Constants of Metal Complexes Database*, program developed by R. J. Mortekaitis, U.S. Department of Commerce, Sept. 1993.

(19) $[\text{Ca}(\text{OH})^+]/[\text{Ca}^{2+}][\text{OH}^-] = 10 \text{ M}^{-1}$. Baes, C. F., Jr.; Mesmer, R. E. *The Hydrolysis of Cations*; John Wiley & Sons: New York, 1976; pp 88–103.

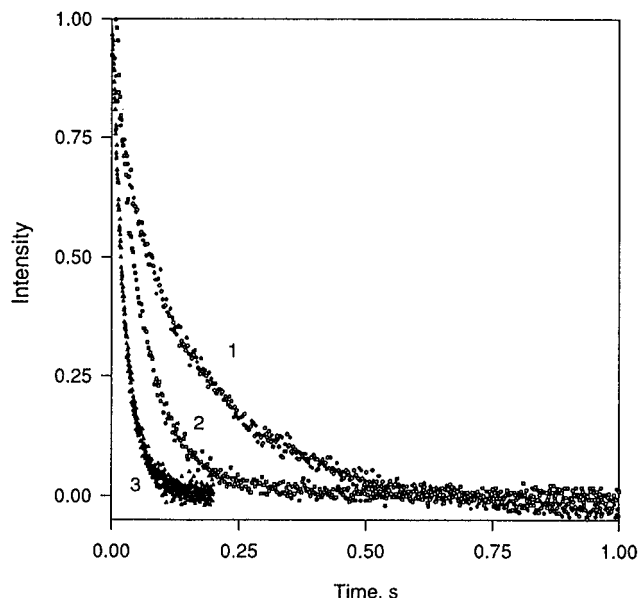


Figure 1. Time course of $\text{Ca}(\text{quin}2)^{2-}$ fluorescence after solutions containing $10 \mu\text{M}$ Ca^{2+} and $40 \mu\text{M}$ $\text{quin}2$ in one syringe are mixed, respectively, with (1) $40 \mu\text{M}$ dota , (2) $160 \mu\text{M}$ dota , and (3) $640 \mu\text{M}$ dota in the second syringe at pH 13.01, 25°C , and $\mu = 0.5 \text{ M}$ ($(\text{CH}_3)_4\text{NCl}$). I_∞ has been subtracted from the data. Note: the concentrations given are before mixing.

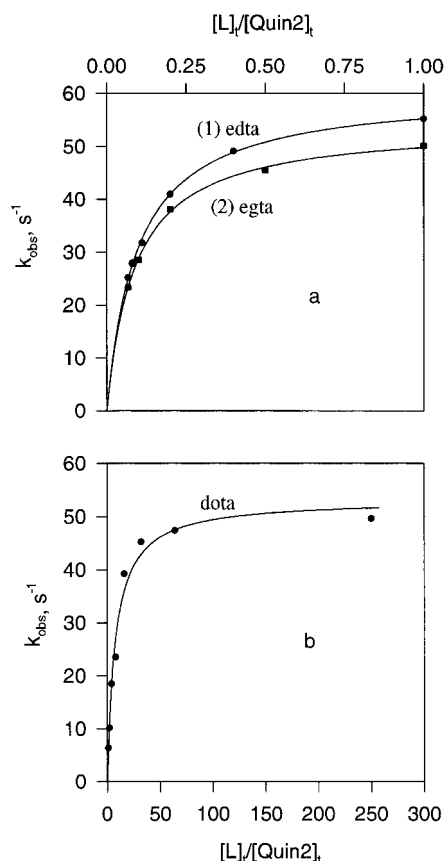


Figure 2. Plots of k_{obs} vs $[\text{L}]/[\text{quin}2]_i$, where L is (a) (1) edta and (2) egta and (b) dota at pH 13.01, 25°C , and $\mu = 0.5 \text{ M}$ ($(\text{CH}_3)_4\text{NCl}$). The curves are hyperbolic least-squares fits to the data.

as the $[\text{L}]/[\text{quin}2]_i$ ratio increases. The fact that large excess concentrations of ligand L do not increase the rate of $\text{Ca}(\text{quin}2)^{2-}$ dissociation shows that the ligand-dependent exchange reaction (eq 5) is negligible under these conditions. Such exchange



reactions become significant only at considerably-higher con-

centrations of L. For example, some NMR studies^{3,20} have shown that the exchange reaction constant between edta^{4-} and $\text{Ca}(\text{edta})^{2-}$ is $74 \text{ M}^{-1} \text{ s}^{-1}$ at 25°C . In the present study the highest ligand concentration used is about 10 mM which leads to an estimate of the pseudo-first-order rate constant of 0.75 s^{-1} , a value negligible when compared to those measured in this study.

Fitting the k_{obs} vs $[\text{L}]/[\text{quin}2]_i$ data to eq 3 yields k_{-2} and k_1/k_2 . The k_{-2} values thus obtained at two pH conditions are 60.6 s^{-1} (edta), 54.3 s^{-1} (egta), 53.1 s^{-1} (dota), and 64.3 s^{-1} (cdta) at pH 13.01 and 59.6 s^{-1} (egta) and 56.6 s^{-1} (edta) at pH 7.01. The average value of k_{-2} found here (58.1 s^{-1}) is in excellent agreement with those reported in the literature (55 – 63 s^{-1}) by different authors.^{15,21}

These same data reveal k_{-1} values near zero (y intercepts, Figure 2). Reported values for these dissociation rate constants are 2.72 , 0.0443 , and 1.0 s^{-1} for $\text{Ca}(\text{edta})^{2-}$, $\text{Ca}(\text{cdta})^{2-}$, and $\text{Ca}(\text{egta})^{2-}$, respectively, at pH 7.^{3,22} Ca^{2+} complexes of the more rigid macrocyclic ligands are even more thermodynamically stable and inert to dissociation, making their k_{-1} values even smaller than those of their acyclic analogs. Thus, the k_{-1} term in eq 3 can be safely neglected in all cases.

Using $k_{-2} = 58.1 \text{ s}^{-1}$ and $k_{-1} = 0$, k_1/k_2 values are obtained from the data and are collected in Table 2 along with the k_{obs} values. The formation rate constant of $\text{Ca}(\text{quin}2)^{2-}$, k_2 , is estimated to be $5.54 \times 10^8 \text{ M}^{-1} \text{ s}^{-1}$ from the dissociation equilibrium constant ($K_d = 104.8 \text{ nM}$ at 0.15 M NaCl)¹⁵ and the dissociation rate constant ($k_{-2} = 58.1 \text{ s}^{-1}$). Using the above estimate for k_2 , values of the apparent formation constants, k_1 , were obtained and are listed in Table 2. The pH dependence of the k_1 values is analyzed in a later section.

Method 2: Measurement of the Fluorescence Intensity of Initially-Formed $\text{Ca}(\text{quin}2)^{2-}$. Reaction of Ca^{2+} with $\text{quin}2$ and the other ligands of interest are completed upon mixing within the dead time of the instrument ($\sim 2 \text{ ms}$). The dissociation processes for both $\text{Ca}(\text{quin}2)^{2-}$ and CaL do not proceed to a significant extent in this short time. Because of this, only the formation processes occur in the system for times less than 2 ms , and dissociation processes are entirely negligible. Under these conditions

$$\frac{d[\text{CaL}]}{d[\text{Ca}(\text{quin}2)^{2-}]_i} = \frac{[\text{CaL}]_i}{[\text{Ca}(\text{quin}2)^{2-}]_i} = \frac{k_1}{k_2} \frac{[\text{L}]}{[\text{quin}2]} \quad (6)$$

where $[\text{CaL}]_i$ and $[\text{Ca}(\text{quin}2)^{2-}]_i$ are the initially-formed ($t < 2 \text{ ms}$) concentrations. With ligand concentrations in large excess, the total calcium concentration, C , is given by $C = [\text{CaL}]_i + [\text{Ca}(\text{quin}2)^{2-}]_i$, so from eqs 4 and 6 one gets eq 7

$$I(0) = k'[\text{Ca}(\text{quin}2)^{2-}]_i = k' \left\{ \frac{C}{1 + (k_1/k_2)([\text{L}]/[\text{quin}2]_i)} \right\} \quad (7)$$

where $I(0)$ is the fluorescence intensity of $\text{Ca}(\text{quin}2)^{2-}$ at $t = 0$. Since both L and $\text{quin}2$ are present in large excess over Ca^{2+} , these concentrations are effectively constant at their total concentrations after mixing. Two different experiments were performed to determine k' . In the first, Ca^{2+} ($10 \mu\text{M}$) in one syringe was mixed with excess $\text{quin}2$ ($320 \mu\text{M}$) in the other, resulting (Figure 3, trace 1) in a horizontal trace of amplitude

(20) Kula, R. J.; Rabenstein, D. L. *J. Am. Chem. Soc.* **1967**, *89*, 552–556.

(21) Bayley, P.; Ahlstrom, P.; Martin, S. R.; Forsen, S. *Biochem. Biophys. Res. Commun.* **1984**, *120*, 185–191.

(22) Smith, P. D.; Liesegang, G. W.; Berger, R. L.; Czerlinski, G.; Podolsky, R. J. *Anal. Biochem.* **1984**, *143*, 188–195.

(23) Delgado, R.; Silva, J. *Talanta* **1982**, *29*, 815–822.

(24) Bryson, A.; Fletcher, I. S. *Aust. J. Chem.* **1970**, *23*, 1095–1110.

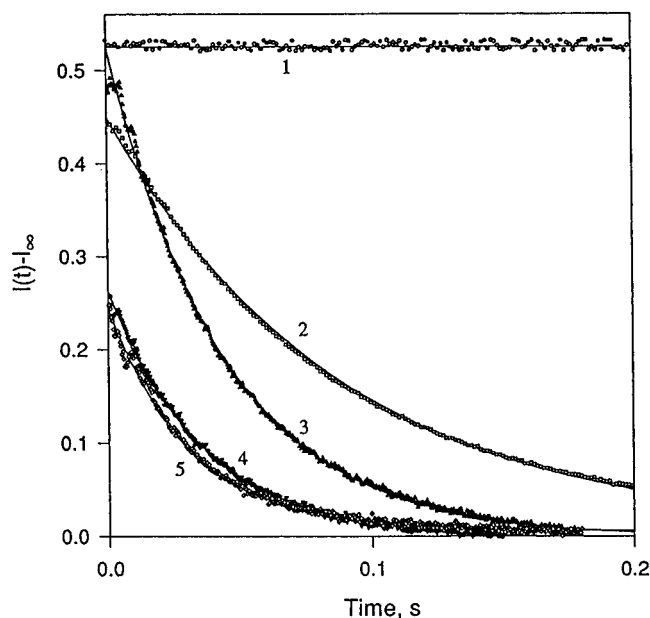


Figure 3. Stopped-flow traces after mixing of 10 μM Ca^{2+} in one syringe with (1) 320 μM quin2; (2) 100 μM quin2 + 1000 μM teta; (4) 360 μM quin2 + 40 μM egta; (5) 320 μM quin2 + 40 μM edta in the second syringe. Trace 3 was recorded after 600 μM quin2 and 10 μM Ca^{2+} in one syringe were mixed with 40 μM egta in the second syringe. For each trace I_∞ has been subtracted. The instrumental conditions were carefully kept constant for all the runs: pH 13.02, 25 $^\circ\text{C}$, and $\mu = 0.5$ M. Note: the concentrations given are before mixing.

$I(0)$. In a second experiment a mixture of Ca^{2+} (10 μM) and quin2 (600 μM) in one syringe was mixed with a solution of another ligand (40 μM egta) (Figure 3, trace 3). The trace in this experiment starts out at $I(0)$ (characteristic of 5 μM $\text{Ca}(\text{quin}2)^{2-}$) and decreases as the dissociation reaction proceeds. The k' values obtained from the above two experiments agree perfectly. The remaining experiments were carried out with various ligands at various pH values (Figure 3, Table S1 in Supporting Information) in order to obtain k_1/k_2 ratios according to eq 8 which follows from eq 7. In these experiments Ca^{2+}

$$\frac{k_1}{k_2} = \left[\left(\frac{k'C}{I(0)} \right) - 1 \right] \frac{[\text{quin}2]_t}{[\text{L}]_t} \quad (8)$$

(10 μM) in one syringe is mixed with a mixture of excess ligand L and quin2 present in known ratios in the other syringe. The $I(0)$ values thus obtained (Figure 3, traces 2, 4, and 5) along with k' values are given in Table 3. The relative formation constants obtained by method 2 are in reasonable agreement with those determined by method 1 and considered to be confirmatory only. The values determined by method 1 are used in the remainder of this paper.

Bimolecular Rate Constants for Reactions of Ca^{2+} with L, HL, and H_2L . The apparent formation rate constants, k_1 , for each CaL complex are plotted as a function of pH in Figure 4. Initially, the k_1 values for all the complexes increase with increasing pH. This finding corresponds to the increase in mole fraction of less protonated forms of the free ligands as the pH increases. At pH values greater than 11, the k_1 values for edta, egta, and teta become approximately constant as expected since $\log K_1$ protonation constants are all less than 11 (Table 1). The k_1 values for these ligands in the pH region 12–13, where hydroxocalcium species become important, are the same as those at pH 11, where $\text{Ca}^{2+}(\text{aq})$ is the predominant metal ion species. This suggests that they represent true values for the formation constant; these values are not significantly affected by the presence of hydrolyzed Ca^{2+} species.

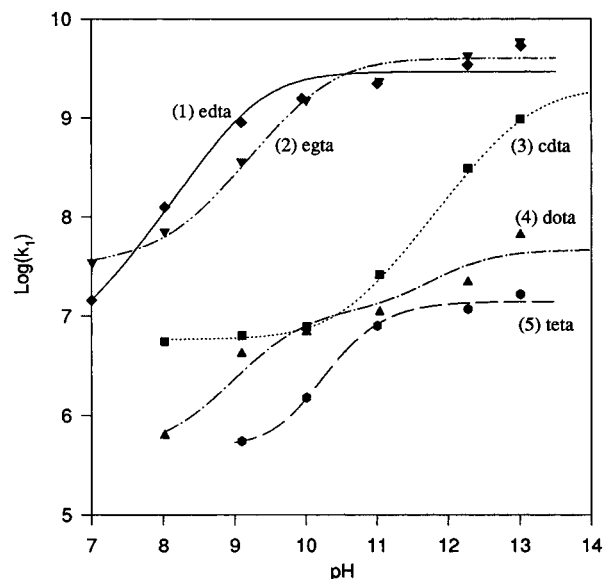


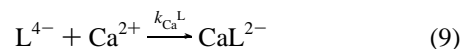
Figure 4. Plots of $\log k_1$ vs pH for Ca^{2+} : (1) edta; (2) egta; (3) cdta; (4) dota; (5) teta systems. The solid curves are the theoretical fits according to eq 12 described in the text.

Table 1. Protonation Constants and Calcium Complex Stability Constants for edta, cdta, egta, do3a, teta, and quin2

ligand	$\log K_1$	$\log K_2$	$\log K_3$	$\log K_4$	$\log K_{\text{CaL}}$
edta ^a	10.22	6.12	2.86	1.8	10.28
cdta ^a	13.09	6.21	3.69	2.63	13.68
egta ^a	9.40	8.78	2.66	2.0	10.86
dota ^b	12.09	9.68	4.55	4.13	17.23
do3a ^c	11.59	9.24	4.43	3.48	
teta ^d	10.85	10.13	4.11	3.27	8.32
quin2 ^e					6.98

^a Reference 3, $\mu = 0.5$ M ($(\text{CH}_3)_4\text{NCl}$), 25 $^\circ\text{C}$. ^b Reference 23, $\mu = 0.10$ M ($(\text{CH}_3)_4\text{NCl}$), 25 $^\circ\text{C}$. ^c Reference 11, $\mu = 0.10$ M ($(\text{CH}_3)_4\text{NCl}$), 25 $^\circ\text{C}$. ^d Reference 18, $\mu = 0.10$ M (R_4NCl), 25 $^\circ\text{C}$. ^e Reference 15, $\mu = 0.15$ M (NaCl), 25 $^\circ\text{C}$.

The sensitivity of the k_1 values to pH in the range pH 7–11 implies a large effect of ligand protonation on formation reaction rates. Over the entire range studied here, the following three species need to be considered: L^{4-} , HL^{3-} , and H_2L^{2-} , which participate in reactions 9, 10, and 11, respectively. Considering



the relevant time scale for the present experiments (k_{obs} values in the range 5–42 s^{-1}), protonation equilibria among free ligand species will be established throughout the course of the complex formation reactions. Thus, the apparent rate constant k_1 may be expressed as eq 12 where $k_{\text{CaL}}^{\text{L}}$, $k_{\text{CaL}}^{\text{HL}}$, and $k_{\text{CaL}}^{\text{H}_2\text{L}}$ are the

$$k_1 = k_{\text{CaL}}^{\text{L}}\alpha_{\text{L}} + k_{\text{CaL}}^{\text{HL}}\alpha_{\text{HL}} + k_{\text{CaL}}^{\text{H}_2\text{L}}\alpha_{\text{H}_2\text{L}} \quad (12)$$

bimolecular rate constants for reactions 9, 10, and 11, respectively, and α_{L} , α_{HL} , and $\alpha_{\text{H}_2\text{L}}$ are the respective distribution functions for a given free ligand.¹⁷ Fitting the data of Figure 4 to eq 12 yields the bimolecular rate constants listed in Table 3 and the computed curves shown in Figure 4. Some literature values are included (in parentheses) for comparison.

Discussion

A two-step process (Eigen mechanism)^{1,2} is generally used to describe the complexation of a metal ion, M, by a ligand,

Table 2. Apparent Rate Constants for the Reaction of Ca²⁺ with dota, do3a, teta, cdta, edta, and egta at Various pH Conditions at 25 °C and $\mu = 0.5$ M ((CH₃)₄NCl), Obtained Using Method 1

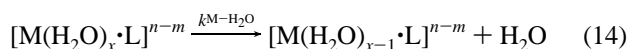
ligand	pH	[quin2]/[L] ($\mu\text{M}/\mu\text{M}$)	k_{obs} (s ⁻¹)	k_1/k_2	k_1 (M ⁻¹ s ⁻¹)
dota	13.01	<i>a</i>		0.12 ± 0.01	(6.7 ± 0.1) × 10 ⁷
	12.28	50/500	17.0 ± 0.1	0.041 ± 0.03	(2.3 ± 0.1) × 10 ⁷
	11/04	50/1000	17.1 ± 0.3	0.021 ± 0.05	(1.2 ± 0.1) × 10 ⁷
	10.01	50/2000	19.6 ± 0.5	0.0127 ± 0.005	(7.1 ± 0.3) × 10 ⁶
do3a	9.10	50/4000	22.1 ± 0.9	0.0077 ± 0.0004	(4.2 ± 0.0) × 10 ⁶
	13.01	20/100	28.0 ± 1.1	0.186 ± 0.1	(1.0 ± 0.1) × 10 ⁸
	12.28	50/250	14.4 ± 0.6	0.066 ± 0.004	(3.7 ± 0.2) × 10 ⁷
	11.04	25/250	5.20 ± 0.1	0.0098 ± 0.0003	(5.5 ± 0.2) × 10 ⁶
teta	10.01	25/500	3.34 ± 0.1	0.00305 ± 0.0001	1.7 ± 0.1 × 10 ⁶
	13.01	50/500	13.6 ± 0.5	0.031 ± 0.002	(1.7 ± 0.1) × 10 ⁷
	12.28	50/1500	22.8 ± 0.6	0.022 ± 0.001	(1.2 ± 0.1) × 10 ⁷
	11.01	50/2000	21.6 ± 0.6	0.015 ± 0.001	(8.2 ± 0.3) × 10 ⁶
cdta	10.01	50/2500	6.86 ± 0.1	0.0027 ± 0.0005	(1.5 ± 0.1) × 10 ⁶
	9.10	50/5000	5.36 ± 0.1	0.0010 ± 0.0003	(5.6 ± 0.2) × 10 ⁵
	13.01	<i>a</i>		1.8 ± 0.1	(1.0 ± 0.1) × 10 ⁹
	12.28	50/50	21.6 ± 1.0	0.59 ± 0.04	(3.3 ± 0.2) × 10 ⁸
edta	11.04	50/100	5.20 ± 0.2	0.049 ± 0.003	(2.7 ± 0.2) × 10 ⁷
	10.01	50/500	7.44 ± 0.2	0.015 ± 0.001	(8.1 ± 0.3) × 10 ⁶
	9.10	50/2000	18.9 ± 0.5	0.012 ± 0.001	(6.7 ± 0.2) × 10 ⁶
	8.02	50/5000	30.0 ± 1.1	0.011 ± 0.001	(5.9 ± 0.3) × 10 ⁶
egta	13.01	<i>a</i>		11.3 ± 0.1	(6.2 ± 0.1) × 10 ⁹
	12.28	160/20	29.9 ± 1.2	8.5 ± 0.5	(4.7 ± 0.3) × 10 ⁹
	11.04	80/20	30.7 ± 1.4	4.5 ± 0.3	(2.5 ± 0.2) × 10 ⁹
	10.01	50/25	34.3 ± 1.2	2.9 ± 0.1	(1.6 ± 0.1) × 10 ⁹
egta	9.10	50/70	28.2 ± 1.0	0.68 ± 0.03	(3.7 ± 0.2) × 10 ⁸
	8.02	50/200	20.0 ± 0.9	0.13 ± 0.01	(7.3 ± 0.5) × 10 ⁷
	7.01	50/1000	31.1 ± 1.1	0.058 ± 0.003	(3.2 ± 0.2) × 10 ⁷
	13.02	<i>a</i>		9.5 ± 0.1	(5.3 ± 0.1) × 10 ⁹
egta	12.28	80/20	35.2 ± 1.1	6.1 ± 0.3	(3.4 ± 0.2) × 10 ⁹
	11.01	80/20	28.9 ± 0.9	4.0 ± 0.2	(2.2 ± 0.1) × 10 ⁹
	10.01	50/25	33.9 ± 1.2	2.8 ± 0.1	(1.6 ± 0.2) × 10 ⁹
	9.10	50/80	41.6 ± 1.1	1.6 ± 0.1	(8.7 ± 0.3) × 10 ⁸
egta	8.02	50/200	27.2 ± 0.5	0.22 ± 0.01	(1.3 ± 0.0) × 10 ⁸
	7.01	50/1000	19.6 ± 0.3	0.025 ± 0.001	(1.4 ± 0.0) × 10 ⁷

^a See data in Figure 2.**Table 3.** Formation Rate Constants of CaL Complexes (25 °C, $\mu = 0.5$ M ((CH₃)₄NCl))

ligand	$k_{\text{Ca}^{\text{L}}}^{\text{L}}$ (M ⁻¹ s ⁻¹)	$k_{\text{Ca}^{\text{HL}}}^{\text{L}}$ (M ⁻¹ s ⁻¹)	$k_{\text{Ca}^{\text{H}_2\text{L}}}^{\text{L}}$ (M ⁻¹ s ⁻¹)
dota	4.7 × 10 ⁷	1.2 × 10 ⁷ (7.9 × 10 ⁵) ^a	4.5 × 10 ⁵
teta	1.1 × 10 ⁷	1.0 × 10 ⁶ (2.3 × 10 ⁵) ^a	4.9 × 10 ⁵
do3a	1.0 × 10 ⁸		
cdta	2.3 × 10 ⁹ (1.4 × 10 ⁹) ^b	6.1 × 10 ⁶ (1.7 × 10 ⁶) ^b	
edta	4.1 × 10 ⁹ (2.4 × 10 ¹⁰) ^b	3.9 × 10 ⁷ (3.7 × 10 ⁷) ^c	
egta	2.1 × 10 ⁹ (<2.5 × 10 ⁹) ^f	7.5 × 10 ⁸ (2 × 10 ⁸) ^d (1.65 × 10 ⁷) ^f	2.2 × 10 ⁶ (1.5 × 10 ⁶) ^e

^a Reference 6. ^b Reference 3. ^c Reference 24. ^d Reference 22, measured at pH 8.4, 25 °C, $\mu = 0.1$. ^e Reference 22, measured at pH 7, 25 °C, $\mu = 0.1$. ^f 35 °C; Mirti, P. J. *Inorg. Nucl. Chem.* **1979**, *41*, 323.

L. Reaction 13 represents the rapid formation of an outer-sphere



complex with an association constant, K_{os} . The rate-determining step, reaction 14, is controlled by the characteristic water exchange constant $k^{\text{M-H}_2\text{O}}$ of the metal ion. This mechanism leads to the formation rate constant k_f given by eq 15. If ligand

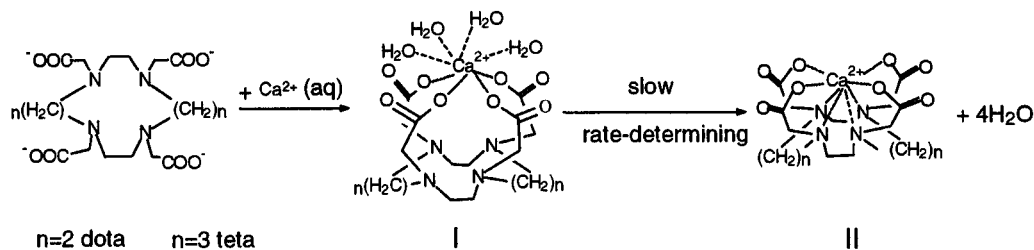
$$k_f = K_{\text{os}} k^{\text{M-H}_2\text{O}} \quad (15)$$

L is multidentate, it is generally assumed that subsequent replacement of first-coordination-sphere water molecules by ligand donor atoms is more rapid than the initial one and $k^{\text{M-H}_2\text{O}}$ is still rate-determining. According to this mechanism the energetics of ligand conformational changes will not affect the rate of complexation. It is instructive, then, to compare the k_f value predicted by eq 15 with actual measurements of this quantity.

On the basis of the Eigen mechanism, Carr and Swartzfager³ predict a $k_{\text{Ca}^{\text{L}}}^{\text{L}}$ value of 2.5×10^{10} M⁻¹ s⁻¹ for the reaction of Ca²⁺ with a ligand of charge -4. Our measurements yield $k_{\text{Ca}^{\text{edta}}}^{\text{L}} = 4.1 \times 10^9$ M⁻¹ s⁻¹, $k_{\text{Ca}^{\text{cdta}}}^{\text{L}} = 2.3 \times 10^9$ M⁻¹ s⁻¹, and $k_{\text{Ca}^{\text{egta}}}^{\text{L}} = 2.1 \times 10^9$ M⁻¹ s⁻¹, which are from about six to ten times smaller than the predicted value. Thus, it appears that the multidentate nature and/or other structural features of these ligands exert a non-negligible effect on the kinetics of complexation. These findings prove that the formation rate constants are not limited solely by the rate of water ligand dissociation.

For the macrocyclic ligands the $k_{\text{Ca}^{\text{L}}}^{\text{L}}$ values are markedly smaller than those of the acyclic ligands. For instance, the measured formation rate constant values for dota, teta, and do3a are smaller by factors of 87, 360, and 39, respectively, than those for $k_{\text{Ca}^{\text{edta}}}^{\text{L}}$ (Figure 4, Table 3). The complexation of many macrocyclic ligands, including those studied here, with labile metal ions (e.g., Ca³⁺, Ln³⁺) have been found to involve rapidly-formed intermediates which convert slowly to the final products.⁵⁻¹³ These slow conversions necessarily involve ligand conformational changes and ligand-dictated first-coordination-sphere rearrangements, the energetics of which are crucial to the rates of these processes. Brücher and Sherry⁸ first proposed,

Scheme 1



in the case of the reaction of Gd³⁺ with the triaza tricarboxylate macrocyclic ligand, nota, that the OH⁻ ion assists in conversion of the intermediate to the final product. Since then OH⁻ ion catalysis of complex formation has been observed in many systems, leading to a general expression for the observed formation rate constant k_{obs} under conditions of a large excess of metal ion, given by eq 16. The rate constant, $k_{\text{H}_2\text{O}}$, for the

$$k_{\text{obs}} = k_{\text{H}_2\text{O}} + k_{\text{OH}}[\text{OH}^-] \quad (16)$$

non-hydroxide-assisted pathway has generally been found to be negligible leading to

$$k_{\text{obs}} = k_{\text{OH}}[\text{OH}^-] \quad (17)$$

The data obtained by a number of authors, generally over a narrow range of pH values below neutrality, fit well to empirical eq 17. In the low pH region partially-protonated forms of these ligands predominate and the intermediates themselves involve protons. Under these conditions hydroxide ion-induced deprotonation dominates the kinetics and obscures other factors, such as ligand structure, which affect the rate-determining conversion of the intermediate into final product.

We earlier pointed out¹² in conjunction with our study of the kinetics of formation of Eu(dota)⁻ that at high pH where neither the free ligand species nor the intermediate can involve protons, the kinetic rate constant should be independent of hydroxide ion concentration. The present study was designed to confirm this prediction and has done so. We also suggested that both the existence of the intermediate itself and the sluggishness of its conversion to final product result from the structure of the macrocyclic ligand which inhibits the facile transit of the metal ion into the binding cavity. It was further suggested that protonation of ring aza nitrogens serves to inhibit their inversion and thereby blocks ligand conformational changes necessary to achieve full coordination of the metal ion. It was projected that the limiting rate constants at high pH values, where deprotonation is not involved, will reflect differences in ligand (and intermediate) structural constraints. This is consistent with the present finding that formation rate constants for the macrocyclic ligands are less than those of their acyclic counterparts.

A kinetic study by Kasprzyk and Wilkins⁶ implicated rapidly-formed intermediates in the reactions of Ca²⁺ with dota and teta in the pH range 7.5–10.4. Our own work provides direct spectroscopic evidence for such intermediates in the case of Eu³⁺ reacting with the same two ligands.^{12,13} On the basis of these findings and the present study, we propose the reaction mechanism (shown in Scheme 1) for Ca²⁺ with dota⁴⁻ or teta⁴⁻. Intermediate I is very rapidly-formed and possesses some degree of stability. The rate-determining step (I → II) is controlled by ligand structural restraints and the energetics of the conformational changes involved in moving the Ca²⁺ into the macrocyclic cavity with the *simultaneous loss of several coordinated water molecules*. Some support for this mechanism is provided by a molecular dynamics simulation which showed, that for the case

of Gd(H₂O)₉³⁺ and dota⁴⁻, the first step in Scheme 1 requires about 1 ps while the second step takes 4 ps.^{25,26} The fact that conversion of I → II requires the near-simultaneous stripping of probably four water molecules from the Ca²⁺ ion is undoubtedly important in determining the rate-limiting barriers. In the case of the Eu³⁺–dota system, the intermediate involves five coordinated water molecules compared with one water in the final complex.¹² Since Ca²⁺ generally exhibits a coordination number smaller by one than that for Eu³⁺, it is likely that the Ca²⁺–dota intermediate involves four water molecules in an 8-coordinate structure (Scheme 1). Ca(dota)²⁻ is known to be 8-coordinate with no waters in the solid state,²⁷ hence the need to simultaneously remove four water molecules in the rate-determining step. For acyclic ligands, no such requirement for simultaneous metal ion dehydration is necessary.

In our previous work¹² it was pointed out that for reactions carried out at pH 6 and below the most stable intermediates found in the reaction of either Eu³⁺ or Ca²⁺ and dota are most likely the diprotonated, [M(H₂dota)]⁺ or ⁰, species. When a proton is removed from such an intermediate, the monoprotonated intermediate becomes poised for conversion to the final product with concomitant expulsion of the final proton. The close correspondence in the present study of the $k_{\text{Ca}}^{\text{dota}}$ and $k_{\text{Ca}}^{\text{Hdota}}$ values (Table 3) lends support to this mechanism.

Finally, it should be noted that while the k_{Ca}^{L} values are roughly equal (within a factor of 2) for all the acyclic ligands (edta, egta, cdta), the $k_{\text{Ca}}^{\text{HL}}$ values range over 2 orders of magnitude with $k_{\text{Ca}}^{\text{Hcdta}} < k_{\text{Ca}}^{\text{Hedta}} < k_{\text{Ca}}^{\text{Hegta}}$ (Table 3). This order correlates with the decreasing difficulty of removal of the final proton from each of the ligands as reflected in their log K_1 values (Table 1).

Conclusions. Apparent formation rate constants, k_1 , for multidentate ligand complexes of Ca²⁺ reach constant maximum values at high pH (11–13), characteristic of their formation from fully-deprotonated ligand species. The bimolecular formation rate constants k_{Ca}^{L} for fully-deprotonated ligands are smaller for macrocyclic ligands than for those of their acyclic counterparts, owing to constraints imposed in the conversion of rapidly-formed intermediates to final products. In the case of macrocyclic ligands this conversion involves ligand conformational changes and the simultaneous stripping or decoordination of several coordinated water molecules from the Ca²⁺ ion.

Acknowledgment. This work was supported by a grant from the National Science Foundation.

Supporting Information Available: An appendix describing the derivation of eq 3 and Table S1, giving kinetics parameters obtained using method 2 (3 pages), is provided. Ordering information is given on any current masthead page.

IC960649Y

(25) Fossheim, R.; Dahl, S. G. *Acta Chem. Scand.* **1990**, *44*, 698–706.

(26) Fossheim, R.; Dugstadt, H.; Dahl, S. G. *J. Med. Chem.* **1991**, *34*, 819–826.

(27) Anderson, O. P.; Reibenspies, J. H. *Acta Crystallogr.* **1996**, *C52*, 792–795.